Chapter 1

Spectrometer systems for radio astronomy

Danny C. Price, Jack Hickish and Dan Werthimer
Campbell Hall 339, UC Berkeley
Address goes here,
dancpr@berkeley.edu

This review gives an introduction to spectrometers and discusses their use within radio astronomy. While a variety of technologies are introduced, particular emphasis is given to digital systems, with details of current-generation implementations given as examples. Three different types of digital spectrometers are discussed: autocorrelation spectrometers, Fourier transform spectrometers, and polyphase filterbank spectrometers. Given their growing ubiquity and significant advantages, polyphase filterbanks are detailed at length. The relative advantages and disadvantages of different spectrometer technologies are compared and contrasted, and implementation considerations are presented.

1. Introduction

A *spectrometer* is a device used to record and measure the spectral content of signals, such as radio waves received from astronomical sources. Specifically, a spectrometer measures the power spectral density (PSD, measured in units of WHz^{-1}) of a signal. Analysis of spectral content can reveal details of radio sources, as well as properties of the intervening medium. For example, spectral line emission from simple molecules such as neutral hydrogen gives rise to narrowband radio signals (Fig. 1), while continuum emission from active galactic nuclei gives rise to wideband signals.

There are two main ways in which the PSD — commonly known as *power spectrum* — of a signal may be computed. The power spectrum, S_{xx}, of a waveform and its autocorrelation function, r_{xx}, are related by the Wiener-Khinchin theorem. This theorem states that the relationship between a stationary (mean and variance do not change over time), ergodic (well-behaved over time) signal $x(t)$, its PSD, and its autocorrelation is given by

$$S_{xx}(\nu) = \int_{-\infty}^{\infty} r_{xx}(\tau) e^{-2\pi i \nu \tau} d\tau. \quad (1)$$

where ν represents frequency, and τ represents a time delay or 'lag'. The autocor-

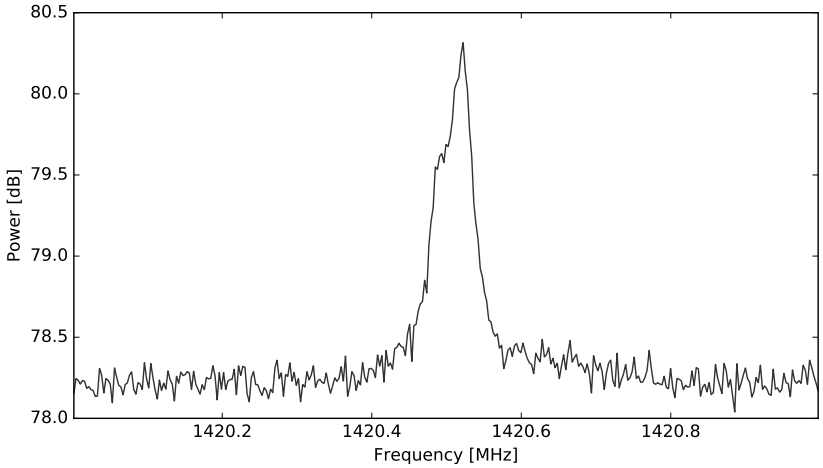

Fig. 1.: A galactic hydrogen 21-cm line emission profile, as measured using a digital spectrometer system on the Robert C. Byrd Greenbank Telescope in West Virginia.

relation function is

$$r_{xx}(\tau) = \langle x(t)x(t-\tau)\rangle\,, \tag{2}$$

where angled brackets refer to averaging over time.

Equation 1 shows that that the autocorrelation function is related to the PSD by a Fourier transform. In the discrete case, the relationship becomes

$$S_{xx}(k) = \sum_{k=-\infty}^{\infty} \langle x(n)x(n-k)\rangle\, e^{-2\pi ik\tau}, \tag{3}$$

which may be recognized as a discrete convolution. It follows from the convolution theorem that

$$S_{xx}(k) = \left\langle |X(k)|^2 \right\rangle, \tag{4}$$

where $X(k)$ denotes the Discrete Fourier Transform (DFT) of $x(t)$:

$$X(k) = \sum_{n=0}^{N-1} x(n)e^{-2\pi ink/N} \tag{5}$$

There are therefore two distinct classes of spectrometers: ones that approximate $S_{xx}(k)$ by firstly forming the autocorrelation, then taking a Fourier transform ala Eq. 3, and those that first convert into the frequency domain to form $X(k)$ before evaulating Eq. 4. We will refer to these as autocorrelation spectrometers (ACS, Sec. 3.1), and Fourier transform filterbanks (FTF, Sec. 3.2), respectively. Polyphase filterbank spectrometers (PFB, Sec. 3.3) can be thought of as an FTF with enhanced filter response.

1.1. *Analysis and synthesis filterbanks*

It is important to note the relationship between spectrometers, filters, and filterbanks. A *filterbank* is simply an array of band-pass filters, designed to split an input signal into multiple components, or similarly, to combine multiple components. These are referred to as *analysis* and *synthesis* filterbanks, respectively. When applied to streaming data, a DFT can be considered an analysis filterbank, and an inverse DFT to be a synthesis filterbank; we return to this in XX. From this viewpoint, a spectrometer is simply an analysis filterbank, where the output of each filter is squared and averaged.

Analysis and synthesis filterbanks have many applications outside of astronomy, see [REF] for further discussion.

1.2. *Polarimetry*

Polarization[14] is a key measurement within radio astronomy. Although most astrophysical radio emission is inherently unpolarized, a number of radio sources — such as pulsars and masers — do emit polarized radiation, and effects such as Faraday rotation by a galactic magnetic fields can yield polarized signals. A spectrometer that also measures polarization is known as a *polarimeter* (or spectropolarimeter).

1.2.1. *Stokes parameters*

The Stokes parameters are a set of four quantities which fully describe the polarization state of an electromagnetic wave; this is what a polarimeter must measure. The four Stokes parameters, I, Q, U and V, are related to the amplitudes of perpendicular components of the electric field:

$$E_x = e_x(t)cos(\omega t + \delta_x) \tag{6}$$
$$E_y = e_y(t)cos(\omega t + \delta_y) \tag{7}$$

by time averages of the electric field parameters:

$$I = \left\langle E_x E_x^* + E_y E_y^* \right\rangle \tag{8}$$
$$Q = \left\langle E_x E_x^* - E_y E_y^* \right\rangle \tag{9}$$
$$U = \left\langle E_x E_y^* + E_y E_x^* \right\rangle \tag{10}$$
$$V = i\left\langle E_x E_y^* - E_y E_x^* \right\rangle \tag{11}$$

where $*$ represents conjugation. The parameter I is a measure of the total power in the wave, Q and U represent the linearly polarised components, and V represents the circularly polarised component. The Stokes parameters have the dimensions of flux density, and they combine additively for independent waves.

1.2.2. *Measuring polarization products*

In order to compute polarization products, a spectrometer must be presented with two voltage signals, $x(t)$ and $y(t)$, from a dual-polarization feed (i.e. a set of orthogonal antennas). With analogy to Eq. 4, we may form

$$S_{xx}(k) = \langle X(k)X^*(k)\rangle = \langle |X(k)|^2\rangle \tag{12}$$

$$S_{yy}(k) = \langle Y(k)Y^*(k)\rangle = \langle |Y(k)|^2\rangle \tag{13}$$

$$S_{xy}(k) = \langle X(k)Y^*(k)\rangle \tag{14}$$

$$S_{yx}(k) = \langle Y(k)X^*(k)\rangle \tag{15}$$

where in addition to measuring the PSD of $x(t)$ and $y(t)$, we also compute their cross correlations. Note that while S_{xx} and S_{yy} are real valued, S_{xy} and S_{yx} are complex valued.

The four terms $\langle E_x E_x^*\rangle$, $\langle E_y E_y^*\rangle$, $\langle E_x E_y^*\rangle$, and $\langle E_y E_x^*\rangle$ are linearly related (by calibration factors) to the quantities in Eq. 12-15 above. Combining these therefore allows for Stokes I, Q, U and V to be determined.

In order to focus on the fundamental characteristics of spectrometers, the remainder of this chapter details single-polarization systems that compute only S_{xx}. Nevertheless, the techniques and characterization approaches are broadly applicable to polarimetry systems.

1.3. *Performance characteristics*

There are several important characteristics to consider when comparing spectrometer implementations. Spectrometers operate over a finite bandwidth B, over which N channels with bandwidth $\Delta\nu = B/N$ are computed. With digital filters, it is possible for each channel to be evenly spaced and to have identical filter shapes.

Ideally, each channel would have unitary response over $\nu_c \pm \frac{\Delta\nu}{2}$, where ν_c is the center frequency, with zero response outside this passband. In practice, this cannot be achieved; each channel has a non-zero response over all frequencies. Fig. 2 compares the normalized filter response for ACS, FTF and PFB implementations. As such, a signal will 'leak' between neighboring channels, known as *spectral leakage*. In the presence of strong narrowband signals, such as radio interference (RFI), spectral leakage is a major concern.

A related concern is that the channel's non-ideal shape will cause narrowband signals at channel edges to be attenuated, an effect known as scalloping loss (Fig. 3). Spectrometers are often designed such that neighboring channels overlap at their full-width at half-maximum points (FWHM), in which case the signal will be spread evenly over both channels. Wideband signals are not affected by scalloping.

Two other important factors are 1) the minimum and maximum integration times, $t_{\min}$ and $t_{\max}$, over which a spectrometer may operate, and 2) the dynamic range (DR), the span of powers over which a spectrometer can operate nominally. These factors are generally enforced by hardware limitations. Detection of transient

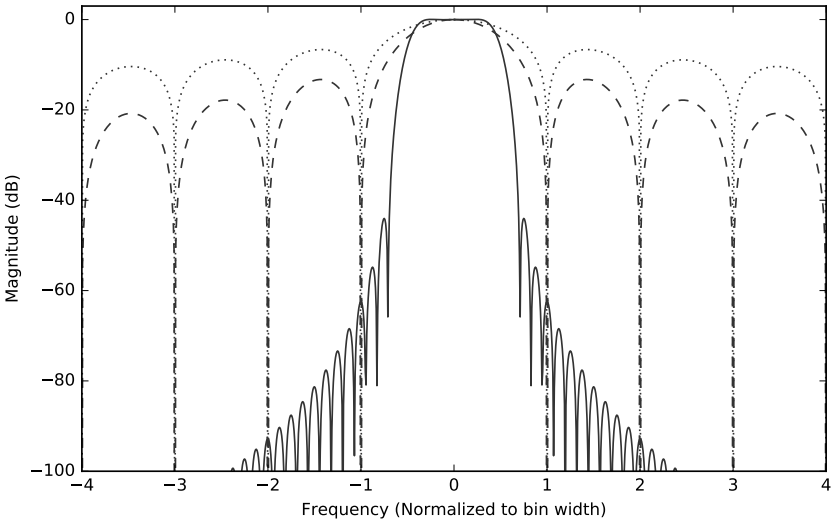

Fig. 2.: Comparison of the filter response of a, ACS (dotted line), FTF (dashed line) and an 8-tap, Hann-windowed PFB (solid line).

phenomena, such as fast radio bursts (FRBs [REF]) and pulsars, require $t_{\min}$ to be as short as a nanosecond; integration lengths of several seconds are common when observing faint sources. The presence of RFI is often the main driver for dynamic range; see Sec. 2.1.4.

PFB spectrometers offer less scalloping loss and spectral leakage than both ACS and FTF implementations. Nevertheless, ACS and FTF systems are still encountered within radio astronomy. Further comparison of architectures is given in Sec. 3.4.

2. Digital systems

Digital signal processing (DSP) techniques are well-suited to applications such as filtering and forming filterbanks; as such, a majority of current-day spectrometers are based on digital technology. A basic understanding of DSP is required to fully understand digital spectrometers; there are several excellent DSP texts available.[?,?]

In the diagrams and equations that follow, the symbol $\otimes$ denotes multiplication of time samples, and $\oplus$ denotes addition. The symbol z^{-n} is used to denote a time delay of n units, due to the relationship between time delay in a digital stream and the z-transform. The symbol $\downarrow D$ is used for downsampling by a factor D and $\uparrow U$ for upsampling by a factor U.

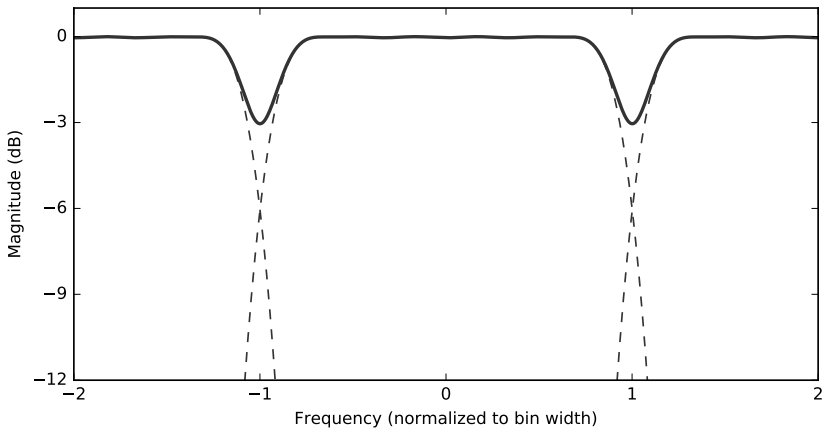

Fig. 3.: Example of scalloping loss between spectrometer channels. The dashed lines show the response of individual channels, while the black line shows the overall response.

2.1. *Digital sampling*

Digital sampling, or digitization, is the process of converting an analog signal to a digital one. As their name implies, analog to digital converters (ADCs) do this conversion. The two main characteristics of an ADC are its sample rate, ν_{s}, and the number of bits per sample, N_{bits}.

2.1.1. *Nyquist sampling*

The ADC converts an analog voltage waveform into a series of numeric quantities called samples. The sample rate determines the amount of bandwidth that can be unambiguously processed by an ADC. The Nyquist Theorem — one of the most fundamental theorems within signal processing — states that a band-limited signal may be fully recovered when it is sampled at a rate that is twice the bandwidth, $\nu_{\mathrm{s}} = 2B$. Sampling at the Nyquist rate is referred to as *critical sampling*, under the Nyquist rate as *undersampling*, and sampling over the Nyquist rate as *oversampling*. Sample rates may be increased by a process known as *upsampling* and decreased by *downsampling*, by using sample rate conversion filters.

Undersampling a signal causes an effect known as *aliasing* to occur, whereby different parts of a signal are indistinguishable from each other, resulting in information loss. Note that oversampling a signal does not increase the information content, but under certain circumstances is advantageous for reducing noise and/or distortion.

Compressed sampling [REF] is a recently discovered technique in which signals that exhibit sparsity can be reconstructed using fewer samples than the Nyquist

Table 1.: Quantization efficiencies η_Q for Nyquist sampling with different bit depths N_{bits}. Table modified from Thompson et. al.[12]

N_{bits}	N_{levels}	ε	η_Q
2	4	0.995	0.88115
3	8	0.586	0.96256
4	16	0.335	0.98846
5	32	0.188	0.99651
6	64	0.104	0.99896
7	128	0.0573	0.99970
8	256	0.0312	0.99991

rate. To date, compressive sampling has not been employed in radio astronomy spectrometers.

2.1.2. *Quadrature sampling*

Quadrature sampling[10] is the process of digitizing a band-limited signal and translating it to be centered about 0 Hz. A quadrature-sampled signal is complex valued, in contrast to real-valued Nyquist sampling. A quadrature-sampled signal has $\nu_s = B$; that is, each complex-valued sample is equivalent to two real-valued samples. Quadrature-sampled signals may have negative frequency components (i.e. below 0 Hz).

A Nyquist-sampled signal $x(t)$ centered at ν_0 can be converted into a quadrature-sampled signal $x'(t)$ by multiplication with a complex phasor $e^{-2\pi i\nu_0 t}$:

$$x'(t) = x(t)e^{-2\pi i\nu_0 t}, \tag{16}$$

which is known as quadrature mixing.

The similarity between the phasor $e^{-2\pi i\nu_0 t}$ and that encountered in a DFT is noteworthy: each channel of a DFT can be seen quadrature mixing the input signal, applying a filter of width B, and then downsampling the signal to a rate $\nu_s = B$.

2.1.3. *Quantization efficiency*

The earliest digital correlators[17] used only two-level sampling (one bit), assigning a value of either +1 or -1. This scheme works remarkably well for weak, noise-dominated signals[a]: for Nyquist-sampled signals, a signal-to-noise ratio of $2/\pi = 0.637$ that of the unquantized signal is achievable [REF VAN VLECK 1966] (see Chapter 8 of TMS[13]). For 2-bit data, one can achieve 88% quantization efficiency, which rises to 98% for 4-bit data. Given these high values for low bit-widths, it

[a]That is, we assume that the probability distribution of the signal is close to Gaussian.

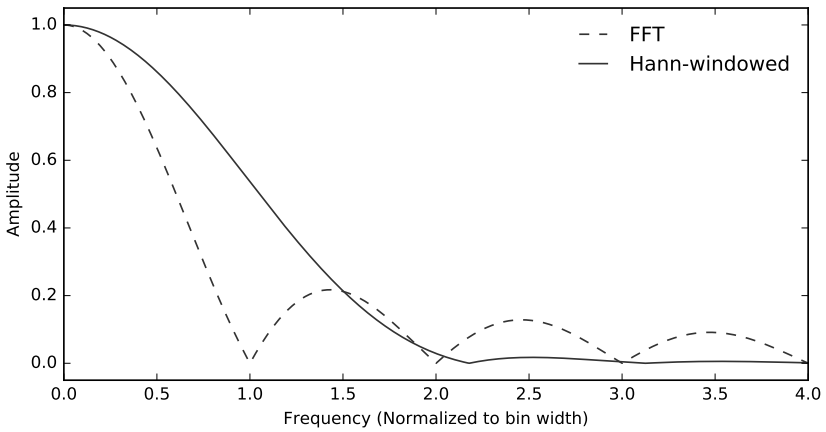

Fig. 4.: Amplitude response of the DFT, compared to amplitude response of a Hann-windowed DFT.

is common to use bits sparingly within radio astronomy applications. A listing of quantization efficiencies[12] is given in Table 1.

Achieving peak quantization efficiency relies on setting the threshold between quantized values optimally. In Table 1, the threshold ε is expressed in units of the signal's standard deviation σ. In order to leave headroom for interfering signals, one may deliberately set ε larger than that optimal for signals with Gaussian probabilities to increase dynamic range.

2.1.4. *Dynamic range*

For modern-day radio environments, RFI is the main driver of sampling bitwidth. RFI may be orders of magnitude stronger than an astronomical signal of interest, requiring a large dynamic range in the digitized waveform. If the maximum input power to an ADC is exceeded, an effect known as *clipping* will occur, in which the waveform is distorted and spurious harmonics are introduced into the digitized waveform.

The theoretical maximum dynamic range of an ADC in decibels is given by

$$DR = 20\ Log_{10}(2^{N_{\text{bits}}}) \approx 6.02 N_{\text{bits}} \tag{17}$$

in practice, as ADCs are imperfect analog devices, their effective number of bits (ENOB) is below this. For example, an 8-bit ADC may have an ENOB of 7.5, resulting in a dynamic range of 45 dB.

2.2. *Windowing functions*

The DFT is computed over a finite number of samples, N, also known as the *window length*. As the window length is not infinite, the response of the DFT is not perfect,

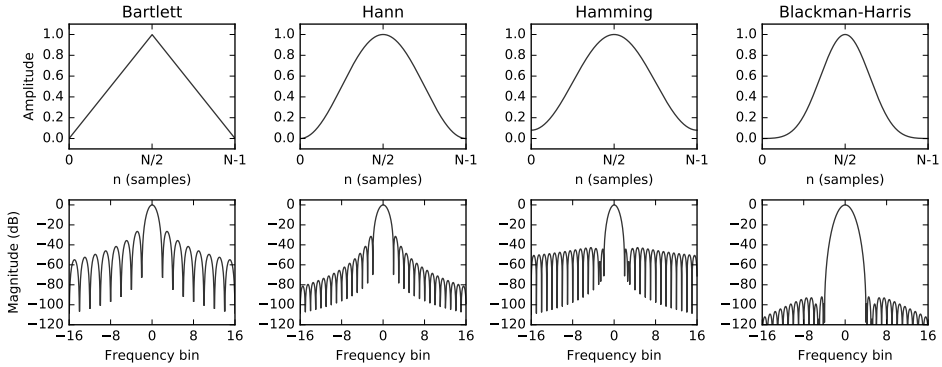

Fig. 5.: Four common windowing functions ($w(n)$, top) and their corresponding squared Fourier transforms ($|W(k)|^2$, bottom). Outside of the range $[0,\, N-1]$, the function $w(n) = 0$ for all windows.

resulting in spectral leakage (Fig. 2). This can be understood if we consider that the DFT

$$X(k) = \sum_{n=0}^{N-1} x(n) e^{-2\pi i n k/N} \tag{18}$$

$$= \sum_{n=-\infty}^{\infty} \Pi(n) x(n) e^{-2\pi i n k/N} \tag{19}$$

$$= \mathcal{F}\{\Pi(n)\} * X'(k) \tag{20}$$

where $\mathcal{F}$ denotes the Fourier transform, and $\Pi(n)$ the rectangle (or tophat) function:

$$\Pi(n) = \begin{cases} 0 & \text{if } n < 0 \\ 1 & \text{if } 0 \leq n \leq N-1 \\ 0 & \text{if } n > N-1, \end{cases} \tag{21}$$

which is Fourier paired with the sinc() function[b]. In other words, we can consider the finite length of the DFT as effectively convolving the perfect Fourier transform response $X'(k)$ with a sinc function. The undesirable peaks of the sinc function are referred to as *sidelobes*.

Windowing functions[7] improve the response of a DFT, by somewhat mitigating sidelobe response, at the expense of increasing the channel width. They are applied by multiplying the signal $x(n)$ by a weighting function, $w(n)$:

$$X_w(k) = \sum_{n=0}^{N-1} w(n) x(n) e^{-2\pi i n k/N} \tag{22}$$

$$= W(k) * X(k). \tag{23}$$

[b]This is the same relationship as that between light passing through a single slit aperture and its far-field diffraction pattern

Table 2.: Some common windowing functions, used in digital filters and DFT filterbanks. Note that in this table, coefficients have been rounded to four significant digits.

Weighting function	$w(n)$
Uniform (rectangular)	1
Bartlett (triangular)	$1 - (\|n\|/(N-1)$
General form:	$a_0 - a_1\ cos(\frac{2\pi n}{N-1})$
Hann	$a_0 = 0.50 \quad a_1 = 0.50$
Hamming	$a_0 = 0.54 \quad a_1 = 0.46$
General form:	$a_0 - a_1\ cos(\frac{2\pi n}{N-1}) + a_2\ cos(\frac{4\pi n}{N-1}) - a_3\ cos(\frac{6\pi n}{N-1})$
Nutall	$a_0 = 0.3558 \quad a_1 = 0.4874 \quad a_2 = 0.1442 \quad a_3 = 0.0126$
Blackman-Nutall	$a_0 = 0.3636 \quad a_1 = 0.4892 \quad a_2 = 0.1366 \quad a_3 = 0.0106$
Blackman-Harris	$a_0 = 0.3588 \quad a_1 = 0.4883 \quad a_2 = 0.1413 \quad a_3 = 0.0117$

The take-home message of all this is that DFT channels have a non-zero response outside their passband (Fig. 4), and that applying a windowing function can improve their response.

Windowing functions are also important in the design of digital filters (Sec. 2.3). Some common windowing functions and their frequency-domain magnitude responses are shown in Fig. 5; their functional forms are given in Tab. 2. The most appropriate windowing function is dependent upon application; for digital spectrometers, the Hamming and Hann windows are commonly applied.

A more dramatic improvement may be achieved by using an lowpass filter frontend before the DFT,[1] to form what is known as a polyphase filterbank. This approach is detailed further Sec. 3.3.

2.3. *Finite impulse response filters*

A finite impulse response (FIR) filter is the windowed moving average of an input sequence $x(t)$. An FIR filter computes the sum

$$y(t) = \sum_{k=0}^{K-1} h(k)x(t-k), \tag{24}$$

where $y(n)$ is the output sequence, and $h(k)$ is a set of K coefficients used for weighting. The upper summation bound, K, is called the number of taps. A streaming implementation of an FIR filter is shown in Figure 6.

If we apply downsampling by $\downarrow D$ to an FIR filtered signal, we only keep the outputs $t = mD$, $m \in \mathbb{Z}^+$. A $\downarrow D$ downsampled filter will alias spectra centered at any multiple of the output sample rate to baseband. In such cases it is more efficient to only compute the terms we wish to keep:

$$y(mD) = \sum_{k=0}^{K-1} h(k)x(mD-k). \tag{25}$$

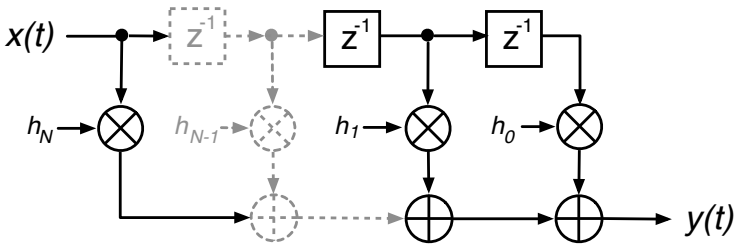

Fig. 6.: N-tap FIR filter block diagram. An FIR filter applies a weighted sum to the input sequence $x(t)$, outputting the filtered signal $y(t)$.

One way we can accomplish this is to use a polyphase decimating filter, which is discussed below.

2.4. *Polyphase FIR filters*

A common technique in DSP is to decompose an input sequence $x(t)$ into a set

$$\mathbb{P} = \left\{x_k(t)\ k \in (0, P-1)\right\} \tag{26}$$

of P sub-sequences, $x_k(t)$, each of which is given by

$$x_k(t) = (\downarrow P)(z^{-k})x(t). \tag{27}$$

This is known as polyphase decomposition. As a simple example, even and odd decomposition of the signal $x(t)$ is achieved when $P = 2$:

$$x_0(t) = \{x(0), x(2), x(4), ...\} \tag{28}$$

$$x_1(t) = \{x(1), x(3), x(5), ...\}\,. \tag{29}$$

More generally, an input stream may be decomposed into P different 'phases'.

Polyphase filter structures are often more efficient than standard finite impulse response filters when used in sample rate conversion. A $\downarrow P$ decimating FIR filter of length $K = MP$ can be constructed from P discrete FIR filter 'branches', each acting upon a different phase; that is

$$y(t) = \sum_{p=0}^{P-1} \sum_{m=0}^{M-1} h_p(m) x_p(t-m), \tag{30}$$

This is known as a decimating polyphase filter. For example, a $P = 4$ branch polyphase filter with $M = 7$ taps per sub-filter would compute the sum

$$\begin{aligned} y(t) = &\sum_{m=0}^{7} h_0(m) x_0(t-m) + \sum_{m=0}^{7} h_1(m) x_1(t-m) \\ &+ \sum_{m=0}^{7} h_2(m) x_2(t-m) + \sum_{m=0}^{7} h_3(m) x_3(t-m), \end{aligned} \tag{31}$$

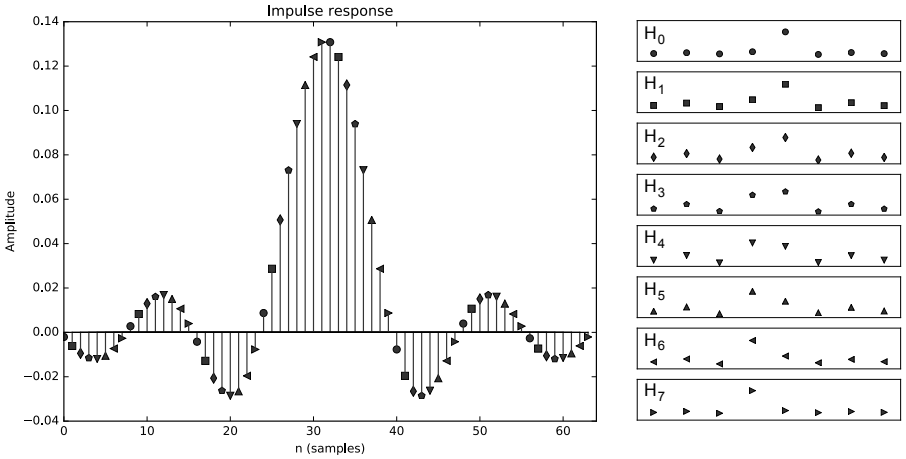

Fig. 7.: Example illustrating the polyphase decomposition of the coefficients h(k) of a 64-tap FIR filter (left) into 8 sub-filters (right). Each sub-filter has 8 taps; that is, P=8 and M=8. These sub-filters may be re-combined in a suitable polyphase filter structure to form a filter with an impulse response equal to the original FIR filter (left).

and has an output equivalent to a $4 \times 7 = 28$ tap standard FIR filter with 4:1 downsampling.

Decimating polyphase filter structures are more efficient than standard FIR filter based downsampling techniques. If $\downarrow D$ downsampling occurs after the moving average of Equation 24, we compute D sums, but keep only 1 in D of these. This is inefficient. In comparison, Equation 30 only computes the output values that are of interest.

A comprehensive overview of polyphase filters is given by Vaidyanathan,[15] and in Chapter 2 of Harris;[?] I will give a brief introduction here.

2.5. *The Fast Fourier Transform*

The Fast Fourier Transform[5] (FFT) is a highly efficient algorithm for computing the DFT of a signal with regularly-spaced samples[c]. To directly compute the DFT

$$X(k) = \sum_{n=0}^{N-1} x(n) e^{-2\pi i n k / N} \tag{32}$$

would require of order $O(N^2)$ operations, but the FFT algorithm reduces this to only $O(N \log_2 N)$ operations. FFT implementations often exhibit best performance

[c]Nyquist and quadrature sampled signals have regularly spaced samples.

when N is a power of 2.

3. Digital spectrometers

The first digital spectrometer used for radio astronomy was developed by Weinreb[17] in 1963. This 1-bit ACS was used to observe the 18-cm wavelength hydroxyl (OH) absorption line in the spectrum of Cassiopeia A, providing the first evidence of OH in the interstellar medium.[16] The first reference to FTF spectrometers for radio astronomy can be found in;[4] however FTF spectrometers did not enjoy widespread adoption until much later. This is due to implementation issues, such as increased data output rates as compared to ACS implementations; see,[3] for a discussion of these issues.

3.1. *Autocorrelation spectrometers*

Regardless of ACS implementation, the PSD (Eq. 1) is computed for only a discrete range of delays, τ. The spacing of lags in an ACS determines how much bandwidth it can process without aliasing occurring. The Nyquist criterion is satisfied when there are two taps per wave period at the highest frequency (shortest wavelength) signal of interest.

Digital autocorrelators implement the autocorrelators delay-and-multiply circuitry using digital delays – shift registers – and digital multiplier cores to compute signal products. As a result, digital correlators can have much more predictable performance than their analog counterparts whose processing is subject to small errors in delay line lengths and other subtle analog effects.

3.2. *Fourier transform spectrometers*

FTF spectrometers compute the PSD of a signal by applying a DFT of length N to an input signal, squaring the DFT output, then taking an average over time.

For a signal with sampling rate $\nu_s = 2B$, each DFT channel has a bandwidth B/N, and a quadrature-sampled output rate of $\nu_s/2N = B/N$. As mentioned in Sec. 2.1.1, the DFT (Eq. 32) may be thought of as the mixing of the input signal with a bank of oscillators, followed by an averaging with a square window function. In effect, this is a simple filterbank. Thinking of the DFT as a filterbank, instead of as a transformation of a time-domain signal into a frequency-domain signal, gives an alternative insight into how a spectrometer works.

For real-sampled data the negative frequencies contain no extra information, so they need not be computed. This leaves a a bank of $N/2$ filters, evenly spaced over a bandwidth $\nu_s/2$.

In general, computing Eq. 32 for each value of ν_0 requires N multiplications, and N additions. Since ν_0 can take N independent values itself, the total cost of implementing a DFT filterbank is N^2 operations per transform. If one transform is

computed for every N samples digitized, then the computation rate is of order $\nu_s N$ operations each second.

The FFT (Sec. 2.5) allows Eq. 32 to be evaluated in $O(N \log_2 N)$ operations, or $\nu_s \log_2 N$ when performed every N samples. With computational savings of order $N/\log 2N$ the FFT is an extraordinarily powerful algorithm, which is used heavily throughout radio astronomy. For a spectrometer of 10^4 channels, the FFT algorithm requires approximately 0.1% as many operations as an autocorrelation spectrometer.

3.3. *Polyphase filterbanks*

The polyphase filterbank (PFB) structure[1,9] was first proposed by Bellanger in 1976. A PFB is a computationally efficient implementation of a filterbank, constructed from an FFT preceded by a prototype polyphase FIR filter frontend. PFB-based spectrometers offer vastly lowered spectral leakage over both ACS and FTF architectures.

The PFB exploits the fact that a lowpass filter with coefficients $h(k)$, can be converted into a quadrature bandpass filter with central frequency $\omega_k = 2\pi\nu$ by multiplying the coefficients by $e^{i\omega_k t}$. That is,

$$h_{bpf}(k) = h(k)e^{i\omega_k t}. \tag{33}$$

Now, suppose we have implemented a decimating lowpass polyphase filter. The output of each branch is

$$y_p(t) = \sum_{m=0}^{M-1} h_p(m)x_p(t-m), \tag{34}$$

where $h_p(m)$ are coefficients from our prototype lowpass filter. If we follow this by a DFT, as in Fig. **??**, we then have

$$Y(k) = \sum_{p=0}^{P-1} y_p(t)e^{-2\pi ikp/P} \tag{35}$$

$$= \sum_{p=0}^{P-1}\sum_{m=0}^{M-1} h_p(m)e^{-2\pi ikp/P}x_p(t-m). \tag{36}$$

Comparing this form to Equation 25 and Equation 33, we recognise that the output of this structure is equivalent to a set of $\downarrow P$ decimating polyphase filters:

$$\mathbb{F} = \left\{h_k(m),\, k \in (0, P-1)\right\} \tag{37}$$

where the central frequency of each filter is shifted by an amount $2\pi ik/P$. For data sampled at the Nyquist rate ν_s, this filterbank consists of N filters spanning $-\nu_s/2$ to $\nu_s/2$, with each filter separated by $\nu_s/2N$.

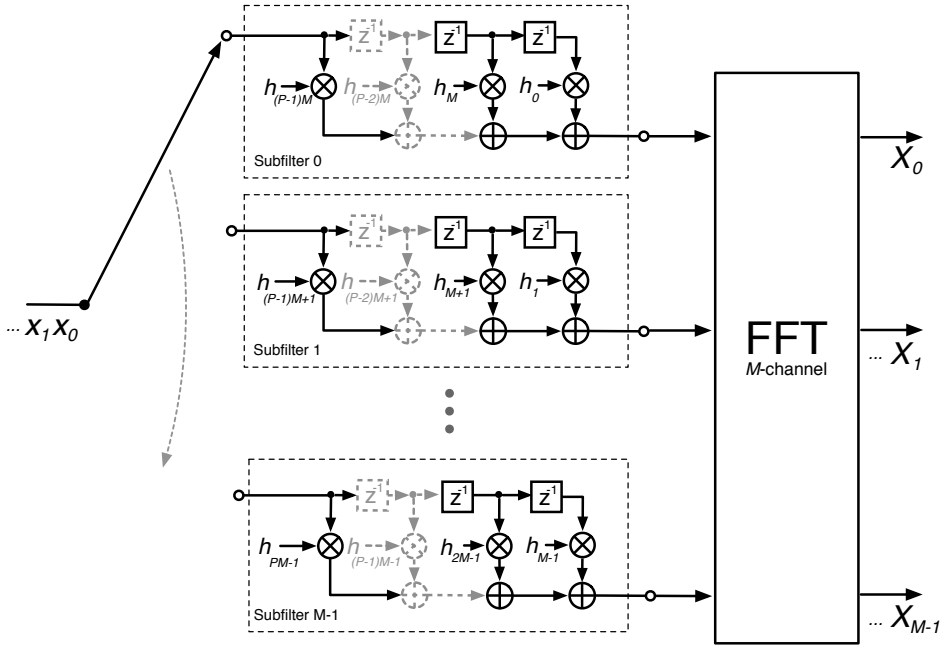

Fig. 8.: Polyphase filterbank streaming implementation.

3.4. *Implementation comparison*

ACS and FTF architectures differ in both their spectral response and the number of computations required to implement them. For regularly sampled data, the Fast Fourier Transform (FFT) algorithm may be used to compute the DFT (see, for example,[2]), which reduces the number of computations required from $O(N^2)$ for to $O(Nlog(N))$. In Chapter 4 of,[11] Romney shows that the ratio of multiplies for the two architectures is

$$R_{\frac{ACS}{FTF}} = \frac{n_t}{2log_2(n_t)}, \tag{38}$$

where n_t is the number of samples per FFT or lag correlation. So in general, FTF architectures require fewer computations than their equivalent ACS counterpart. Romney also shows that the spectral response of FTF and ACS architectures differ, with ACS architectures having a *sinc* reponse, and FTF architectures posessing a $sinc^2$ response. The result is that interchannel isolation is better in FTF architectures (first sidelobe at ~ -13.6 dB), than in ACS architectures (~ -6.8 dB).

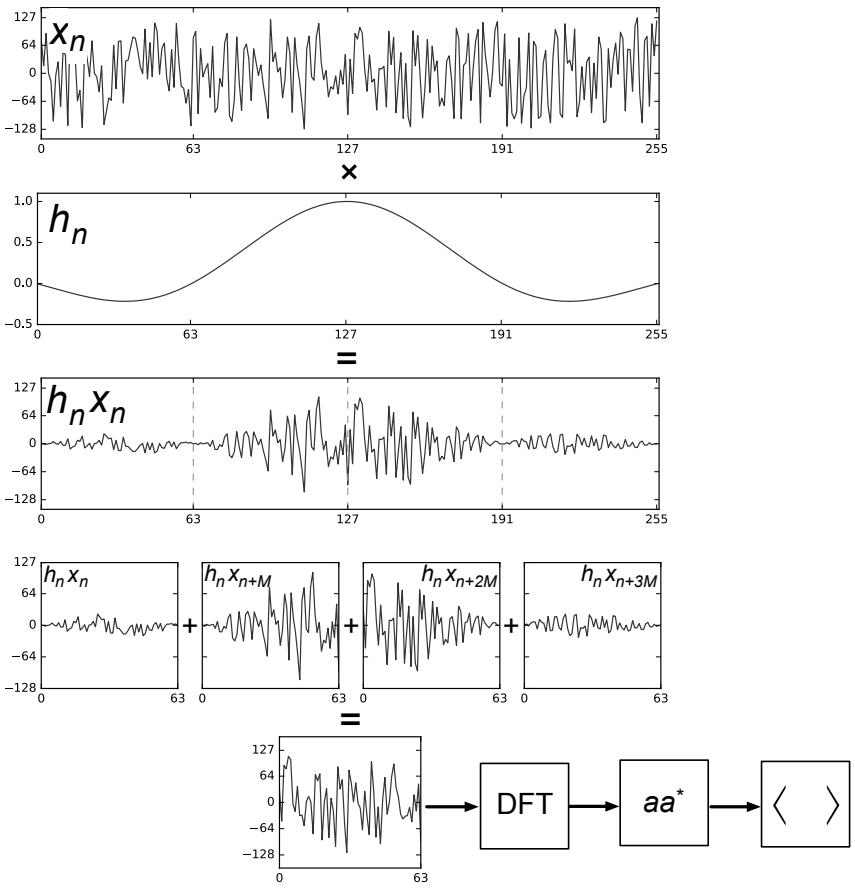

Fig. 9.

3.5. *Zoom modes*

4. Alternative spectrometer implementations

4.1. *Swept spectrometer*

A *swept spectrometer* uses a variable oscillator with a heterodyne circuit and a low pass filter. The oscillator is typically varied, i.e. swept, through a range of desired frequencies. As it is swept through the desired frequency range, the power of the low pass filter's output is measured and recorded. Most analog spectrum analyzers operate in this manner.

An advantage of swept spectrometers is that they can operate over large RF bandwidths. However, as only a fraction of the band is detected at any one time,

less integration time is available per frequency channel. For a swept spectrometer with N channels with a sweep time of t_{sweep}, the integration time available per channel is t_{sweep}/N. It follows that the RMS noise per channel is $\sqrt{N}$ higher than an equivalent filterbank spectrometer covering the entire RF bandwidth. As such, swept spectrometers are best suited for cases where signals of interest are strong and wideband.

4.2. *Analog filterbank*

An analog filterbank is just what its name implies: a bank (or collection) of analog filters. The analog filters are designed to pass through different ranges of frequencies. The power of the analog filters' output is measured and recorded. By creating a bank of filters with adjacent and non-overlapping passband frequencies one can get a complete picture of the input signal's spectrum.

Analog filterbanks can offer very wide bandwidths, but design of very narrow-band filters is challenging. Additionally, the input signal must be split multiple times, and each time the signal is split, its power is halved. Unlike digital systems, the shape and gain of each filter may differ. For these reasons, analog filterbanks are uncommon in modern radio astronomy.

4.3. *Analog autocorrelator spectrometers*

An analog ACS uses analog circuitry to implement multipliers and propagation times through carefully constructed delay lines to implement the desired tap delays. Details of specific scientific deployments of analog autocorrelation spectrometers can be found in[6] and.[8]

The main advantage of the analog autocorrelator over its digital counterpart (Sec. 3.1) is that digitization need only take place at a rate commensurate with the averaging period of the correlator, rather than the bandwidth of the input signals. For this reason, analog autocorrelation spectrometers are usually seen in systems that have instantaneous bandwidths of many gigahertz which cannot be readily digitized by commercially available ADCs. In contrast, the number of physical components required scales with the number of channels, making analog ACS systems with many channels — readily implemented by digital systems — infeasible.

5. Design considerations and examples

5.1. *Calibration requirements*

Dicke switching and calibration. Other data products: spectral kurtosis.

Jansky and Temperature

5.2. *Time and frequency standards*

5.3. *Telescope metadata*

5.4. *File formats*

5.5. *Current technology*

* table of digitizers
  * FPGA, CPU and GPU comparison
  What's Available Commercially

- GPU
- CPU
- ASIC
- FPGA
- Heterogeneous

5.6. *GnuRadio*

5.7. *CASPER Hardware*

* Fast Readout Spectrometers for Pulsar Timing and Search
  * Multibeam spectrometer systems

5.8. *Example implementations*

* HIPSR * Effelsberg? * Breakthrough listen

6. Conclusions

Polyphase filterbanks have attractive characteristics for radio astronomy applications. They offer excellent interchannel isolation and can be implemented using efficient FFT based structures. Field Programmable Gate Arrays are a viable platform on which to implement wide bandwidth polyphase filterbank spectrometers. I have implemented such a spectrometer using the Xilinx toolflow and CASPER block libraries. In this chapter I detailed the implementation and presented results on its performance.

7. Acknowledgements

The authors thank members of the CASPER collaboration for sharing their extensive knowledge with the wider community. D. Price thanks J. Moran for thorough discussion and debate on the virtues of polyphase filterbanks.

References

1. M Bellanger, G Bonnerot, and M Coudreuse. Digital filtering by polyphase network:application to sample-rate alteration and filter banks. *Acoustics, Speech and Signal Processing, IEEE Transactions on*, 24(2):109 – 114, 1976.
2. E. Oran Brigham. *The FFT and its applications*. Prentice-Hall Inc., 1988.
3. John Bunton. An improved fx correlator. *Alma Memorandum Series*, (342), December 2000.
4. Yoshiro Chikada, Masato Ishiguro, Hisashi Hirabayashi, Masaki Morimoto, and Koh-Ichiro Morita. A 6 x 320-mhz 1024-channel fft cross-spectrum analyzer for radio astronomy. *IEEE*, 75:1203, Sep 1987.
5. James W Cooley and John W Tukey. An algorithm for the machine calculation of complex fourier series. *Mathematics of computation*, 19(90):297–301, 1965.
6. N. Erickson, G. Narayanan, R. Goeller, and R. Grosslein. An Ultra-Wideband Receiver and Spectrometer for 74–110 GHz. In A. J. Baker, J. Glenn, A. I. Harris, J. G. Mangum, and M. S. Yun, editors, *From Z-Machines to ALMA: (Sub)Millimeter Spectroscopy of Galaxies*, volume 375 of *Astronomical Society of the Pacific Conference Series*, page 71, October 2007.
7. Svend Gade and Herkik Herlufsen. Use of weighting functions in dft/fft analysis (part i). *Brüel & Kjær, Windows to FFT Analysis (Part I) Technical Review*, (3), 1987.
8. Andrew I. Harris, K. G. Isaak, and Jonas Zmuidzinas. Wasp: wideband spectrometer for heterodyne spectroscopy, 1998.
9. Christopher Harris and Karen Haines. A Mathematical Review of Polyphase Filterbank Implementations for Radio Astronomy. *Publications of the Astronomical Society of Australia*, 28(4):317–322, October 2011.
10. R Lyons. Quadrature signals: complex, but not complicated. *URL: http://www dspguru com/info/tutor/quadsig htm*, 2000.
11. G. B Taylor, C. L. Carilli, and R. A. Perley, editors. *Synthesis Imaging in Radio Astronomy II*, volume 180. Astronomical Society of the Pacific, 1999.
12. A. R Thompson, D. T Emerson, and F. R Schwab. Convenient formulas for quantization efficiency. *Radio Science*, 42:3022, Jun 2007.
13. A. Richard Thompson, James M. Moran, and George W. Swenson Jr. *Interferometry and Synthesis in Radio Astronomy*. WILEY-VCH Verlag, second edition, 2004.
14. Jaan Tinbergen. *Astronomical Polarimetry*. Cambridge University Press, 2005.
15. Vaidyanathan. Multirate digital filters, filter banks, polyphase networks, and applications: a tutorial. *Proceedings of the IEEE*, 78(1):56 – 93, 1990.
16. S Weinreb, A. H Barrett, M. L Meeks, and J. C Henry. Radio observations of oh in the interstellar medium. *Nature*, 200:829, Nov 1963.
17. Sander Weinreb. A digital spectral analysis technique and its application to radio astronomy. *MIT Research Laboratory of Electronics Technical report*, Jan 1963.